Probabilistic Fracture Mechanics Assessment of BWR Control Rod Drive Penetrations

M. P. Manahan, Sr.[1] and R. B. Stonesifer[2]

1) MPM Technologies, Inc., 2161 Sandy Drive, State College, PA 16803 USA
2) Computational Mechanics, Inc., 1430 Steele Hollow Road, Julian, PA 16844 USA

ABSTRACT

This paper presents results from a probabilistic fracture mechanics (PFM) assessment of boiling water reactor (BWR) control rod drive penetration stub tubes. In particular, the Nine Mile Point Unit 1 (NMP-1) stub tube leak history was analyzed to demonstrate that the PFM model could accurately simulate the stub tube leak trend. The model was then used to determine the probability of experiencing additional leaks in the future. It has been shown that the cause of a large number of leaks early in reactor life (4.3 effective full power years (EFPY)) was due primarily to exposure of the sensitized Type 304 stainless steel to high conductivity water during the first four fuel cycles. The model predicts an expected future leak rate of about 2 stub tubes per startup if the plant is operated under normal water chemistry (NWC) conditions with conductivity below 0.2 : S/cm. This leak rate agrees with plant experience averaged over the past 8 cycles which were run with low conductivity water. On the other hand, if the plant is run under hydrogen water chemistry (HWC), only two new leaks are predicted over the next 14 EFPY of operation.

INTRODUCTION

NMP-1 has experienced leakage problems as the result of stress corrosion cracking in control rod drive (CRD) penetration stub tubes in the reactor pressure vessel (RPV) lower head (see Figure 1). These Type 304 stainless steel stub tubes were shop welded to the vessel head and were therefore subjected to the post weld heat treatment of the vessel. This heat treatment resulted in the stub tubes being furnace sensitized. The field welds attaching the CRD housings to the stub tubes resulted in welding residual stresses in the stub tubes, which when combined with the sensitized state of the tube and the reactor water chemistry, have led to through wall cracking and leakage at 29 out of 129 stub tubes.

A roll repair has been developed and implemented to stop leakage from the stub tubes which have experienced through wall cracking [1]. The rolling process stops leakage by plastically expanding the CRD housing so that upon completion of the rolling, compressive residual radial stresses exist between the housing and the low alloy steel head material. A typical roll region is shown in Figure 1. Ten of the 29 leaking tubes were detected and repaired during the 1984 outage. The second most numerous repairs (7) were made during the 1992 outage. The repairs ranged from 0 to 3 during the remaining outages since the first repairs in 1984. The roll repair history is summarized in Table 1. Visual inspections were performed when the first leaking stub tubes were discovered in 1984. These inspection tapes show intergranular stress corrosion cracking (IGSCC) on the outer surface of the stub tubes. An important issue related to tube roll repair is whether a re-roll would be expected to be effective in case a previously rolled stub tube develops a leak.

A PFM analysis of the NMP-1 stub tube IGSCC problem was undertaken to provide an explanation for the large number of leaks which occurred at the end of cycle 4 and to assess the likelihood of a similar event in the future. As part of the PFM work, finite element modeling was used to calculate welding residual stresses and operating stresses in the stub tube and CRD housing assemblies. Using these models and stresses, stress intensity factor solutions for stub tube cracks were also developed [2]. A special purpose PFM computer program was written to simulate the cracking and leak behavior of the 129 stub tubes. This monte carlo based software implements both the GE crack growth model [3] and the BWR Vessel and Internals Project (BWRVIP) model [4] and allowed conductivity and electrochemical corrosion potential (ECP) histories to be input. The PFM software generates plots of cumulative leaks and new leaks as a function of EFPY of operation. When applying the results to the plant, the difference between hot operation time and EFPY must be taken into account. Comparisons between the actual and predicted leak histories were used to help select those PFM analysis inputs for which data was not available.

PFM MODEL DESCRIPTION

The monte carlo simulation process amounts to randomly selecting inputs from assumed statistical distributions, calculating outputs from the inputs in a deterministic manner, and then repeating the process many times while keeping track of the fraction of the total number of simulations for which a given result occurs. Enough simulations are done so that the statistical distributions of the results change by less than some selected convergence criterion. The basic procedure for leak determination was to model the growth or arrest of a randomly selected set of initial stub tube and housing defects through
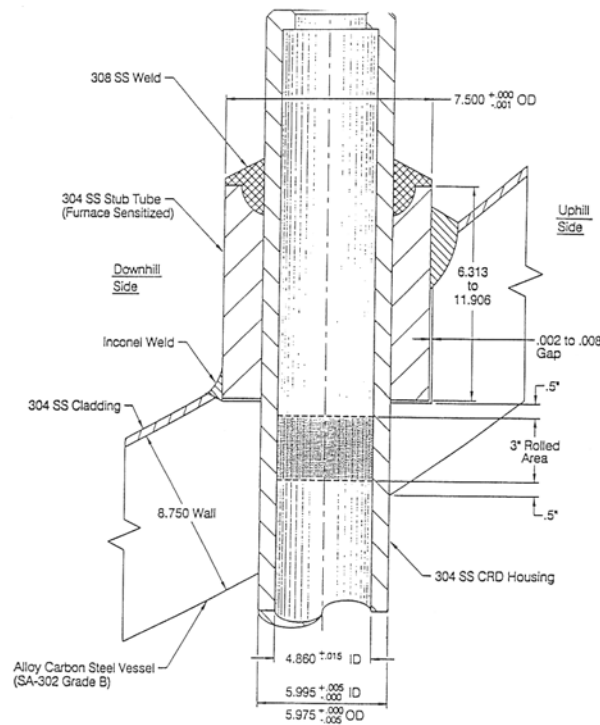
Figure 1   Stub Tube and CRD Housing Assembly with Roll Repair (not drawn to scale) [5]

Table 1   Nine Mile Point Unit 1 Stub Tube Roll Repair History

date	End of Cycle	EFPY	New Leaks	Cumulative Leaks
	3	3.33	0	0
Apr-84	4	4.34	10	10
Aug-86	5	5.81	1	11
Mar-88	6	7.29	0	11
Jun-90	7	8.70	3	14
Oct-91	8	10.27	1	15
Jun-92	9	11.62	7	22
Apr-93	10	13.28	2	24
Mar-95	11	14.78	2	26
Mar-97	12	16.76	3	29

one plant life of 32 EFPY. Then a new set of defects were randomly selected and the analysis repeated. By repeating this process many times (~1000 plant life simulations) and saving the fraction of all simulations which resulted in some behavior of interest (e.g., N or more new leaks in year Y), it was possible to compute a probability for the occurrence of that behavior.

The monte carlo calculation procedure contains six nested loops. The outermost loop is the loop on the number of plant life simulations. This loop is exited when enough plant life simulations have been completed that all solution statistics (e.g., the mean and standard deviation of the number of N new leaks in year Y) have changed by less than an input tolerance. The next loop is the loop over each of the 129 stub tubes. For each stub tube, a number of defects is randomly chosen based on the input control parameters. The next loop is the loop over the number of chosen defects for the current stub tube. For each defect, a depth and circumferential length is randomly chosen based on user inputs. Then, the circumferential position of the defect is randomly chosen. Based on the particular tube being considered, and the circumferential location of the defect, the appropriate stress distribution is determined. The range of stub tube geometry effects were approximated using three axisymmetric models to represent three annular regions in the bottom vessel head. The effects of the non-perpendicular

nature of the actual stub tube axes (relative to the sloping vessel head) on residual stresses were approximated by varying the distance that the stub tube extends beyond the inner vessel wall in each of the three models. Next, based on input parameters, the stress distribution is perturbed by random shifting and scaling. The next step is to loop over the 32 EFPY plant life. Each defect is grown in one EFPY intervals with predicted crack size behavior being saved for each year. After all defects of a tube are simulated, then the leak history of the stub tube can be determined and saved.

After the crack growth behavior for the stub tube is computed, the crack growth behavior of the housing can be simulated. Since IGSCC cannot occur without a corrosive environment, it is assumed that defects in the housing will not begin to grow until the stub tube leaks. The same steps described above for randomly selecting defects, selecting stresses, simulating crack growth, and storing crack size and leak history are then applied to the housing. After convergence of crack depth and leak statistics (mean and standard deviation for each year) is achieved, the leak and crack size data accumulated from all of the simulations can be processed to determine probabilities of crack size and leaks in any given year. These probabilities enable the computation of the median new and cumulative leak histories and their associated 95% confidence ranges.

MODEL INPUTS

The inputs to the simulation can be organized into four categories. The first category includes those inputs which are reasonably well known and for which no statistical variations need to be modeled. The stub tube and housing geometries, the stub tubes that were subjected to a weld cap repair, and the operating loads fall into this category. The second category of inputs are those which are reasonably well known but which have some less well known statistical variation. Inputs of this category are water chemistry and welding residual stresses. The third category contains those which are not well known and which also have some relatively unknown statistical variation. Inputs of this type are the initial defect depth, initial defect aspect ratio, and the number of defects per tube or housing. The final category of inputs are those which do not fit within any of the previous three categories. These include the crack growth model, the assumption on circumferential growth behavior, and the assumption of a threshold K_I for IGSCC.

The approach to selecting the uncertain inputs was to initially select what seemed to be reasonable statistical distributions for each such input and then to run the simulation to get a predicted cumulative stub tube leak history. By graphically superimposing the actual cumulative leak history on the predicted leak history, it was then possible to adjust the various inputs so as to improve the fit between the model predictions and the data. By trial and error, various combinations of inputs were found that provided reasonable fits to the actual cumulative leak history. In this way, the past leak history was used to filter out combinations of inputs that would otherwise be considered reasonable. Since leak data was available for about half of the total 32 EFPY history, this filtering process was effective. Of the cases that matched the leak history, bounding cases in terms of the number of new leaks per year of additional operation were identified.

The key inputs to the monte carlo simulation which involve random selection from an assumed statistical distribution are: conductivity; ECP; residual plus operating stress distribution; number of defects per tube; initial defect depth; and initial defect length to depth ratio. Key inputs to the simulation which do not involve a random selection are: crack growth law; threshold K_I for IGSCC; and circumferential growth assumption. Details concerning the input distributions are provided in References [2] and [6]. One input of particular importance, which will be discussed briefly, is the time dependent conductivity. As in the case of several older BWRs, the first few fuel cycles were operated at a high conductivity level. By the mid-1980s, it was widely recognized that conductivity is a primary variable in IGSCC of 304 SS and most plants took steps to clean up their primary system water. In the case of NMP-1, the average conductivity over the first 5 fuel cycles was high and ranged between 0.4 μS/cm and 0.6 μS/cm for 1 to 5 EFPY of operation. After about 11 EFPY, the average conductivity has been kept below 0.1 μS/cm.

PFM SIMULATION RESULTS

Figure 2 shows the predicted worst case new leak history resulting from a PFM simulation that used what is believed to be a reasonable and realistic set of inputs. This predicted history has a peak for new leaks per EFPY in the period 5 to 9 EFPY. The 95% confidence range for new leaks in this period is about 1 to 8 leaks per EFPY with an expected number of 3 or 4. By EFPY 10, the 95% confidence range on new leaks is 0 to 5 leaks, with the median expected number of new leaks being about 2 new leaks per year. The leak behavior at year 10 is predicted to continue through EFPY 32. The predicted cumulative leak behavior associated with the new leak behavior of Figure 2 is shown in Figure 3. It can be seen that the predicted behavior is in good agreement with the actual leak behavior. Other baseline PFM analyses that also reasonably fit the leak data suggest a gradual decline in the rate of new leaks to as few as one new leak per EFPY.

The same monte carlo simulation that resulted in the cumulative leak behavior of Figure 3 also predicted that most stub tube cracks grew to more than 40% of the stub tube wall thickness by EFPY 17 (approximately the current time). Due to small net compressive axial stresses from operating loads, and the tendency for crack growth to relieve tensile residual stresses, many of these cracks tended to arrest before growing through wall. By EFPY 32, the average crack depth for all
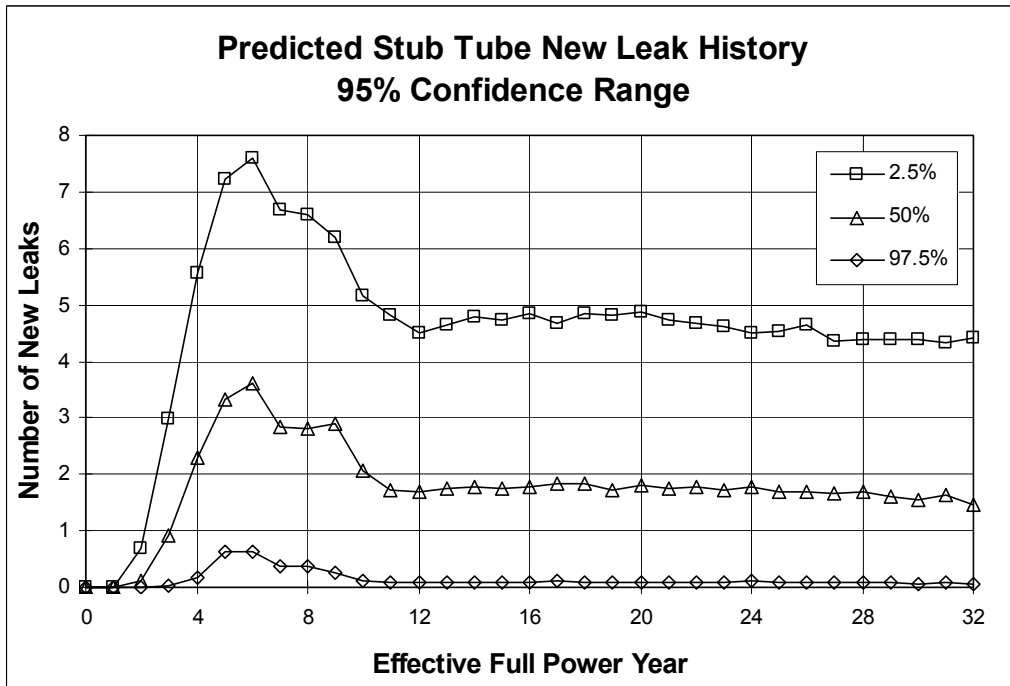
Figure 2 Predicted Stub Tube Leak Behavior Showing Higher Rates of New Leaks in Early Years and a Steady Lower Rate of New Leaks in Later Years (baseline Case 1)
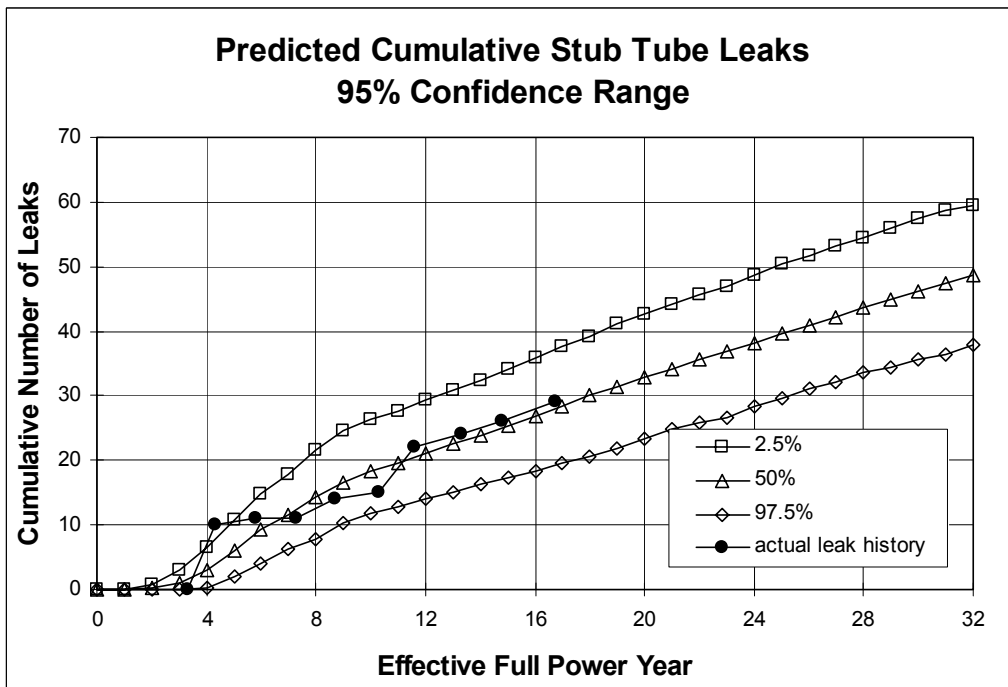

Figure 3 Comparison of Actual and Predicted Stub Tube Cumulative Leak Behavior (baseline Case 1)

cracks is expected to be about 55% of the wall thickness. The average depth of the deepest crack from each of the 129 stub tubes was predicted to be over 90% through wall by EFPY 17.

Parametric analyses were performed on the key input parameters and these results are reported in [6]. These analyses led to the conclusion that the initial large number of leaks (10 leaks at the end of cycle 4) resulted from the high conductivity early in plant life. To illustrate this effect, an analysis was preformed assuming that the current water chemistry was present since initial startup. The model predicted only five leaking stub tubes by 32 EFPY. The results of Figure 3, which show good model agreement with the cumulative leaks, were obtained using the actual plant conductivity data.

Two levels of hydrogen injection were simulated. It was assumed in both cases that hydrogen injection would be started at the beginning of EFPY 19. The predicted leak behavior for the "full hydrogen injection" case is shown in Figure 4. The predicted leak behavior for a "partial hydrogen injection" case was also analyzed. The "full hydrogen injection" case predicts only one new leak during the last 14 EFPY of operation. The "partial hydrogen injection" case is almost as beneficial, with only about two new leaks predicted for the last 14 EFPY of operation. The PFM model clearly illustrates the significant benefits of HWC.

The PFM analyses of this study included crack growth in the CRD housings. It was assumed that crack growth would not initiate in a housing until its stub tube leaked, thus subjecting the housing J weld crevice heat-affected zone (HAZ) to a corrosive environment. The PFM model represented the fact that the J weld only results in sensitization at the housing outer surface due to its not being a full penetration weld. For housing crack growth, only the first 1/8 inch of wall thickness was assumed to be sensitized.

The baseline PFM analyses (i.e., 50% probability) of this study predicted no through wall housing cracks by EFPY 32. Of the three baseline cases, the worst case housing behavior was a 3% chance of one leak by EFPY 32. The lack of predicted through wall cracks in the housings was due to the much lower assumed growth rates in non sensitized base metal. As mentioned earlier, the sensitized material (EPR of 15 C/cm^2) was assumed to extend 0.125 inches from the housing outer surface. The material below the sensitized material was assumed to be stainless steel base metal with an EPR of 0 C/cm^2. When sensitized material growth rates were conservatively assumed for the entire housing material thickness, 2 housing leaks were predicted by EFPY 17, and 7 housing leaks were predicted by EFPY 32.
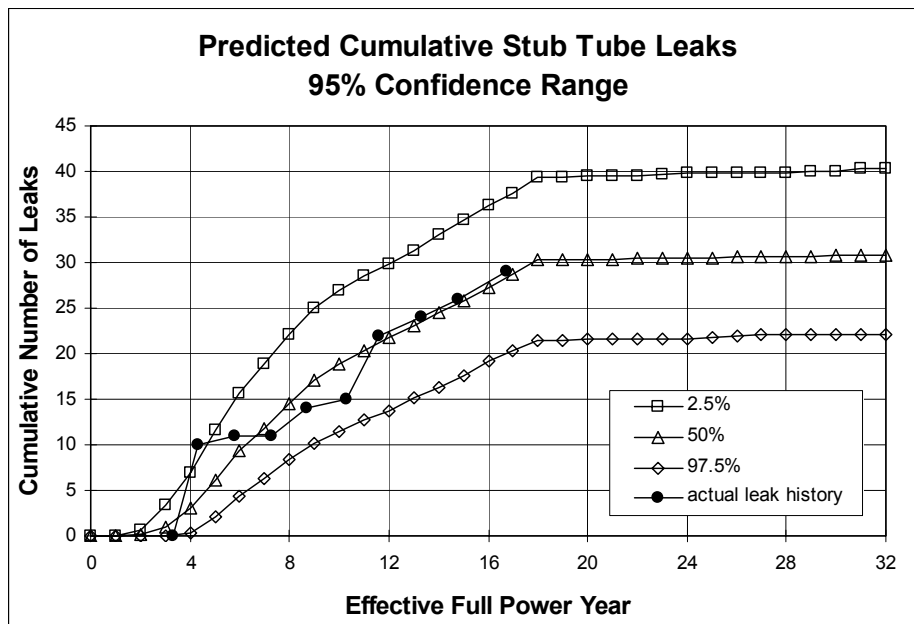

**Figure 4   Predicted Stub Tube Leak Behavior for "full hydrogen injection" Starting in EFPY 19**

ROLL REPAIR SIMULATIONS

Simulations of the roll repair process were used to predict the residual interface compression between the expanded housing and the vessel wall. The results of these simulations were compared to results given in the recent report prepared by the BWRVIP Repair Committee and MPR Associates [7]. The rolling model used in [7] is based on an analytical model developed in 1943 [8]. The developers of this model made the assumptions that the materials do not harden during plasticity and, more importantly, that unloading from the fully expanded state involves only elastic material behavior. The authors of

5

[8] were fully aware that the assumption of entirely elastic unloading was faulty but at that time the authors had no reasonable alternative. This shortcoming of their model resulted in their not being able to explain the experimental observation that expansion beyond some optimum level is detrimental. A key factor in the final residual interface compression due to rolling is the Bauschinger effect that is exhibited by type 304 stainless steel. "Bauschinger effect" is the name given to the tendency for a metal to yield at a lower stress level upon reverse loading than during the initial loading and was first described in the literature by Bauschinger in 1886 [9]. To include a Bauschinger effect, a rolling model must be able to correctly model plasticity behavior during the unloading phase of the rolling operation. Since the Reference [8] model assumed elastic unloading, no Bauschinger effect could be included.

   In the current study, any plastic behavior during unloading was correctly modeled. Several representative stress-strain curves were considered in order to better understand the sensitivity of the results to key modeling assumptions and material variability. The case of no Bauschinger effect (isotropic hardening) was considered as well as maximum Bauschinger effect (kinematic hardening). The isotropic hardening cases generally provided results that were in fair agreement with those of [7,10,11]. Kinematic hardening, which is generally believed to be a much better representation of actual Type 304 stainless steel material behavior, predicted residual interface contact pressures that were sensitive to the assumed stress-strain curve. The differences in the interface residual stress results tended to be amplified by the consideration of operating conditions since the operating loads tend to reduce the interface's compressive stress level. The geometric complexity of the stub tube assembly requires 2D finite element modeling, as used in this study, to reasonably treat pressure and thermal loads. Previous studies appear to have relied entirely on handbook solutions for operating load effects.

   Figure 5 shows stress-strain curves that demonstrate the variability of Type 304 stainless steel. The three "ORNL" curves are based on data compiled in [12] that show heat-to-heat variability. The curve with circular points is a bilinear fit to the "EPRI NP-1931" curve [13] for strains in the 0 to 2% range. The curve with square points is representative of that which was used in the rolling simulations of [10].   The rolling repair process is designed to achieve a set amount of wall thinning in the housing. The target for initial repairs is 4% wall thinning. If a previously repaired tube develops a new leak, a second rolling can be done for a total wall thinning of 6%. Based on these thinning levels, stress-strain behavior in the 4 to 6% strain range is considered to be of primary importance in the simulations.
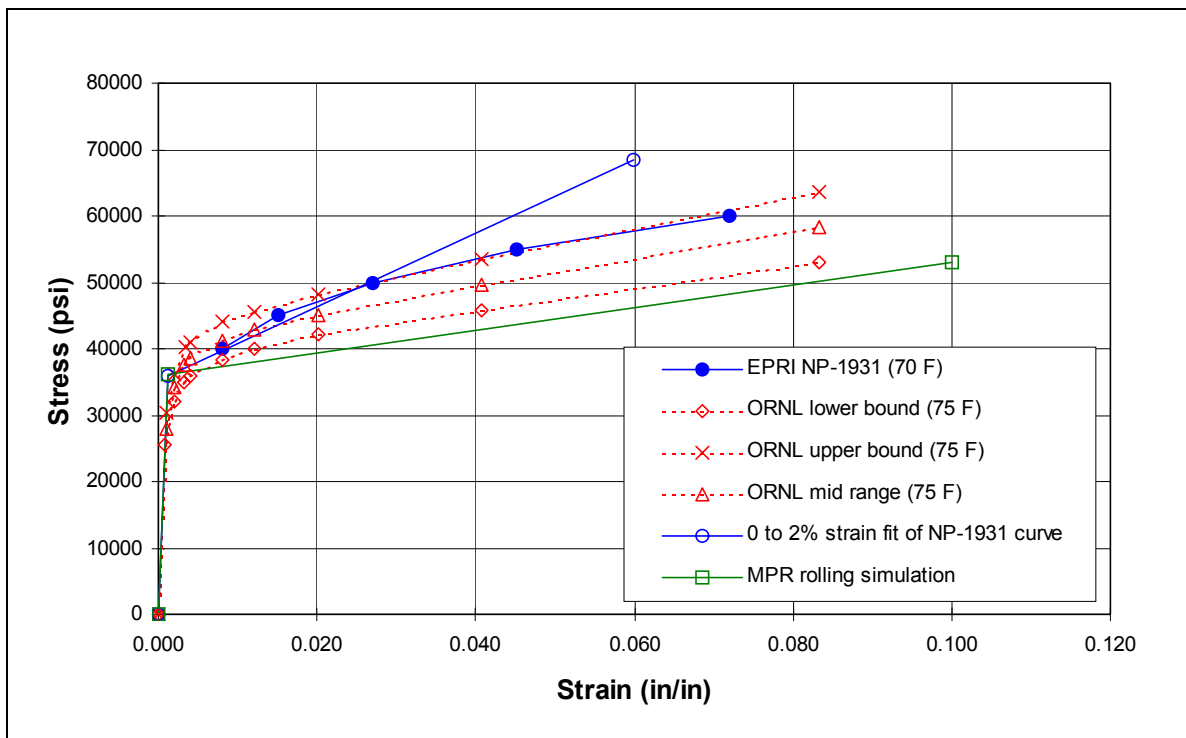
Figure 5   Stress-Strain Curves for Type 304 Stainless Steel Used in the Rolling Simulations

   Figure 6 shows the as-rolled interface residual stresses from simulations based on the stress-strain curves of Figure 5. All of the plotted cases assumed kinematic hardening. It can be seen from Figure 5 that the ORNL stress-strain curves are bounded by the MPR curve and the bilinear fit of the NP-1931 curve in the critical 3% to 6% strain range. In Figure 6,

however, the interface stress results from the ORNL stress-strain curves are not bounded by the interface stress results of the MPR and NP-1931 bilinear fit. This unexpected result shows that the interface stress is affected independently by two aspects of the stress-strain curve. One aspect is the magnitude of the stress at a given reference strain of interest and the other is the slope of the stress-strain curve in the strain range of interest. For a bilinear stress-strain curve, the two parameters are simply the yield stress and the hardening modulus. Figure 6 also contains results that show the repair results are not sensitive to the initial gap size.
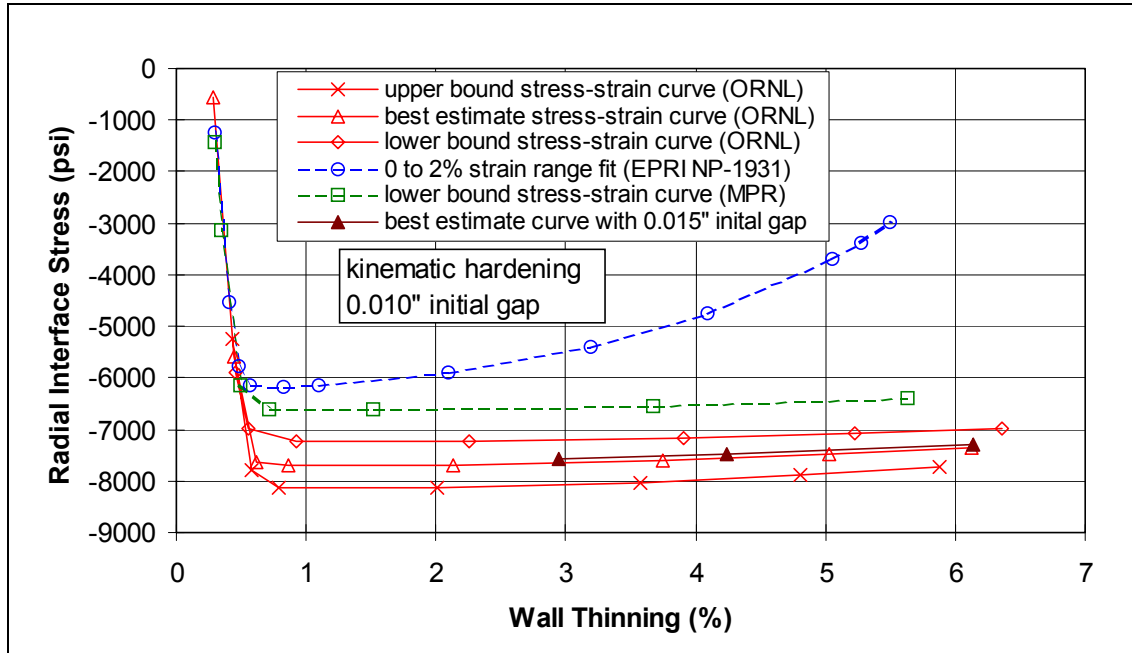

Figure 6   Rolling Repair Induced Radial Interface Stress for Several Stress-Strain Curve Assumptions

SUMMARY AND CONCLUSIONS

The PFM analyses have resulted in robust conclusions concerning the likelihood of stub tube leaks at NMP-1 in the future. All of the PFM simulations indicate that the peak in new leaks per year has passed. The large number of leaks that occurred at the end of fuel cycle 4 was the result of high conductivity in the first few plant cycles. The predicted best and worst case behaviors differ by about one new leak per EFPY. Therefore, it is predicted that the new leak behavior for the remaining plant life will be similar to, and perhaps slightly better than, that of the past several years. The simulations definitely indicate a tendency for the arrest of IGSCC cracks before through wall cracking occurs. This tendency for arrest is the result of the small net compressive axial stress acting on the stub tube during operation. The water chemistry improvement that has occurred since initial startup has had the effect of slowing crack growth. The overall conclusion is that PFM is a very effective tool for assessing future system performance in cases where failure history data are available. The data can be used to find realistic ranges and combinations of uncertain variables by seeking those that result in the model matching the historical performance. This process also naturally leads to bounding of the predicted behavior.

The predicted residual interface compression after application of operating pressure and thermal loads is shown in Figure 7 to be in the −3 to −5.5 ksi range. It is therefore concluded that the 4% wall thinning roll repair should stop leaks. The plan to reroll to a total 6% wall thinning if a tube leaks a second time also appears viable. The predicted interface compression range is consistent with the three to five times system pressure that was considered to be a requirement for an effective roll repair by the BWRVIP [7]. The consistency between the current predicted interface stress levels and those of [7] that were based on a primitive mechanics model that does not include strain hardening or Bauschinger effects, and does not reflect the geometric complexity of the stub tube geometry in the calculation of the operating pressure and thermal stresses, while gratifying, is nonetheless a bit surprising.
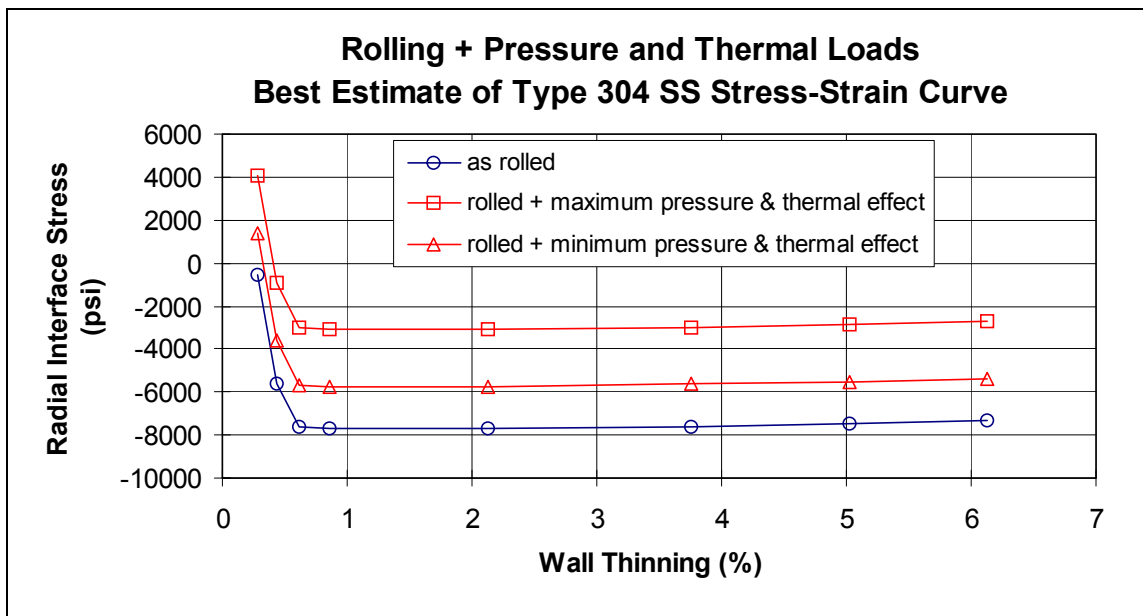
AKNOWLEDGEMENT

Figure 7   Rolling Repair Induced Radial Interface Stress for As-rolled and for Bounding Operating Conditions

REFERENCES

1 . "Control Rod Drive (CRD) Housing Rolling", Nine Mile Point Nuclear Station Unit 1, Mechanical Maintenance Procedure, N1-MMP-044-659, Revision 2, April 1997.

2 . "Nine Mile Point Unit 1 Stub Tube Probabilistic Fracture Analysis Phase 2", final report prepared by MPM Technologies, Inc. for Niagara Mohawk Power Corporation, MPM-1099407, September 1999.

3 . Jones, R.H., "Stress-Corrosion Cracking", ASM International.

4 . "Evaluation of Crack Growth in BWR Stainless Steel RPV Internals", BWR Vessel and Internals Project, EPRI Report TR-105873, 1996.

5 . Niagara Mohawk Power Co., RFQ R209719, July 2, 1996.

6 . "Nine Mile Point Unit 1 Stub Tube Probabilistic Fracture Analysis", final report prepared by MPM Technologies, Inc. for Niagara Mohawk Power Corporation, MPM-796401, December 1996.

7 . "Roll/Expansion Repair of Control Rod Drive and In-Core Instrument Penetrations in BWR Vessels", BWR Vessel and Internals Project, (BWRVIP-17), prepared by BWRVIP Repair Committee and MPR Associates, EPRI TR-106712, November 1996.

8 . Goodier, J. N., and Schoessow, G. J., "The Holding Power and Hydraulic Tightness of Expanded Tube Joints: Analysis of Stress and Deformation", ASME Transactions, July, 1943.

9 . Bauschinger, J., "On the Change of the Elastic Limit and Hardness of Iron and Steels through Extension and Compression, through Heating and Cooling, and through Cycling", Mitteilung aus dem Mechanisch, Technischen Laboratorium der K. Technische Hochschule in München 13, Part 5, 31, 1886.

10 . "Finite Element Analysis of Control Rod Drive (DRD) Penetration Roll Repair Process", report prepared by MPR Associates for Niagara Mohawk Power Corporation, April 19, 1988.

11 . "Reactor Pressure Vessel Control Rod Drive (CRD) Penetration Repair Program", report prepared by MPR Associates for Niagara Mohawk Power Corporation, MPR-847, November 2, 1984 (See Appendix D).

12 . "Heat-to-Heat Variations of Total Strain (to 5%) at Discrete Stress Levels in Types 316 and 304 Stainless Steel from 24 to 316 °C", prepared for the U. S. Nuclear Regulatory Commission by the Oak Ridge National Laboratory, ORNL/NUREG/TM-57, April 1997.

13. "An Engineering Approach for Elastic-Plastic Fracture Analysis", report NP-1931, Project 1237-1, report prepared for Electric Power Research Institute by General Electric Company, July, 1981.